

4. CONCLUSIONS

To improve the efficiency of the PBSV-DDM, we employ a set of orthogonal polynomials to approximate the Robin-type transmission conditions. It was shown that, with the proposed method, the computational cost and the memory requirements of the PBSV-DDM can greatly be decreased. More importantly, compared with the rank-revealing factorization, e.g., ACA, based DDM, a remarkable feature of the proposed method is that the compression of the PBSV matrix can be achieved without obtaining the entire matrix in advance.

ACKNOWLEDGMENTS

This work was supported in part by the National Science Foundation of China under Grant 60801039.

REFERENCES

1. C. Farhat and F.X. Roux, A method of finite element tearing and interconnecting and its parallel solution algorithm, *Int J Numer Methods Eng* 32 (1991), 1205–1227.
2. B. Després, Domain decomposition method and the Helmholtz problem. II, In: *Second International Conference on Mathematical and Numerical Aspects of Wave Propagation*, Newark, DE, 1993, SIAM, Philadelphia, PA, 1993, pp. 197–206.
3. A domain decomposition method for the harmonic Maxwell equations, In: *Iterative Methods in Linear Algebra*, Elsevier, Amsterdam, Netherlands; Philadelphia, PA, 1992, pp. 475–484.
4. B. Stupfel and M. Mognot, A domain decomposition method for the vector wave equation, *IEEE Trans Antennas Propag* 48 (2000), 653–660.
5. C. Farhat, M. Lesoinne, P. LeTallec, and K.P.D. Rixen, FETI-DP: A dual-primal unified FETI method—Part I: A faster alternative to the two-level FETI method, *Int J Numer Methods Eng* 50 (2001), 1523–1544.
6. W. Hong, X.X. Yin, X. An, Z.-Q. Lü, and T.J. Cui, A mixed algorithm of domain decomposition method and the measured equation of invariance for the electromagnetic problems, *IEEE Antennas Propag Soc Intl Symp* 3 (2004), 2255–2258.
7. S.-C. Lee, M.N. Vouvakis, and J.-F. Lee, A non-overlapping domain decomposition method with non-matching grids for modeling large finite antenna arrays, *J Comput Phys* 203 (2005), 1–21.
8. Y. Li and J.-M. Jin, A vector dual-primal finite element tearing and interconnecting method for solving 3-D large-scale electromagnetic problems, *IEEE Trans Antennas Propag* 54 (2006), 3000–3009.
9. M. Vouvakis, Z. Cendes, and J.-F. Lee, A FEM domain decomposition method for photonic and electromagnetic bandgap structures, *IEEE Trans Antennas Propag* 54 (2006), 721–733.
10. X. An and Z.-Q. Lü, A fast algorithm based on partial basic solution vectors domain decomposition method for scattering analysis of electrically large cylinders, *J Comput Phys* 219 (2006), 930–942.
11. K. Zhao, V. Rawat, and J.F. Lee, A domain decomposition method with non-conformal meshes for finite periodic and semi-periodic structures, *IEEE Trans Antennas Propag* 55 (2007), 2559–2570.
12. Z.-Q. Lü, X. An, and W. Hong, A fast domain decomposition method for solving three-dimensional large-scale electromagnetic problems, *IEEE Trans Antennas Propag* 56 (2008), 2200–2210.
13. J.M. Jin, *The finite element method in electromagnetics*, 2nd ed., Wiley, New York, 2002.
14. M. Bebendorf, Approximation of boundary element matrices, *Numerische Mathematik* 86 (2000), 565–589.
15. K. Zhao, M. Vouvakis, and J.-F. Lee, The adaptive cross approximation algorithm for accelerated method of moments computations of EMC problems, *IEEE Trans Electromagn Compat* 47 (2005), 763–773.

SMALL-SIZE WIDEBAND MONOPOLE ANTENNA CLOSELY COUPLED WITH A CHIP-INDUCTOR-LOADED SHORTED STRIP FOR 11-BAND WWAN/WLAN/WiMAX OPERATION IN THE SLIM MOBILE PHONE

Kin-Lu Wong and Cheng-Tse Lee

Department of Electrical Engineering, National Sun Yat-Sen University, Kaohsiung 80424, Taiwan; Corresponding author: wongkl@ema.ee.nsysu.edu.tw

Received 9 May 2010

ABSTRACT: A small-size wideband antenna suitable for the 11-band WWAN/WLAN/WiMAX operation in the slim mobile phone is presented. The wideband antenna has a simple structure and is formed by a printed monopole closely coupled with a chip-inductor-loaded shorted strip. The antenna occupies a small footprint of $15 \times 20.5 \text{ mm}^2$ ($\sim 308 \text{ mm}^2$) on the system circuit board and can generate two wide operating bands for the desired 11-band operation. The antenna's upper band is mainly contributed by the printed monopole and covers the GSM1800/1900/UMTS operation (1710–2170 MHz), the 2.4/5.2/5.8 GHz WLAN operation (2400–2484/5150–5350/5725–5875 MHz), and the 2.5/3.5/5.5 GHz WiMAX operation (2500–2690/3300–3800/5250–5850 MHz). The lower band is contributed by the parasitic chip-inductor-loaded shorted strip closely coupled by the printed monopole and covers the GSM850/900 operation (824–960 MHz). Further, the antenna can be disposed on the system circuit board of the mobile phone with a small thickness of 3 mm only, allowing the antenna very promising to be applied in the modern slim mobile phone. Detailed results of the proposed antenna are presented. The specific absorption rate results of the antenna, including the case with the user's hand presence, are also analyzed. © 2010 Wiley Periodicals, Inc. *Microwave Opt Technol Lett* 53:361–366, 2011; View this article online at wileyonlinelibrary.com. DOI 10.1002/mop.25712

Key words: mobile antennas; internal mobile phone antennas; WWAN antennas; WLAN antennas; WiMAX antennas

1. INTRODUCTION

It has been a continuous challenge in the design of wideband or multiband internal antennas with the attractive features of small size, simple structure, and easy fabrication for the mobile phone applications. In addition, for applications in the modern slim mobile phone, the applied internal antennas should also be of thin thickness, which is generally required to be less than ~ 3 mm [1–5]. To achieve small size, easy fabrication, and wideband operation, the on-board printed internal antennas such as the printed inverted-F antennas or shorted monopole antennas using a coupling feed for five-band WWAN operation [6–10] are attractive for the modern slim mobile phone applications. These coupled-fed antennas are suitable to be directly printed on the system circuit board of the mobile phone and are easy to fabricate at low-cost. Two wide operating bands can also be provided to cover the five-band WWAN operation of GSM850/900/1800/1900/UMTS (824–960/1710–2170 MHz).

However, to achieve decreased near-field emission for the internal WWAN antennas such that the decreased specific absorption rate (SAR) [11] can be obtained, it is proposed that the antenna structure should be as simple as possible. This is because generally the simpler structure of the antenna can lead to smaller slope discontinuity in the excited surface current distributions of the antenna, which in turn can result in decreased near-field emission [12]. For this purpose, we propose in this

article, a wideband on-board internal mobile phone antenna that not only occupies a small size on the system circuit board but also shows a simpler structure than the reported wideband coupled-fed WWAN mobile phone antennas [6–10]. The proposed antenna is a simple printed monopole antenna closely coupled with a parasitic chip-inductor-loaded shorted strip. The antenna occupies a small footprint of $15 \times 20.5 \text{ mm}^2$ on the system circuit board and is easy to fabricate at low-cost as the reported wideband coupled-fed WWAN mobile phone antennas [6–10]. In addition, the antenna can generate two wide operating bands covering not only the five-band WWAN operation but also the three-band (2.4/5.2/5.8 GHz) WLAN operation (2400–2484/5150–5350/5725–5875 MHz) [13–15] and the three-band (2.5/3.5/5.5 GHz) WiMAX operation (2500–2690/3300–3800/5250–5850 MHz) [16–19]. That is, the proposed antenna can cover the 11-band WWAN/WLAN/WiMAX operation. Further, the antenna can be disposed on the system circuit board of the mobile phone with a small thickness of 3 mm only, which makes the antenna very promising to be applied in the modern slim mobile phone.

Detailed operating principle of the proposed antenna is described in this article. The antenna is also fabricated and tested. The obtained results are presented and studied. Also, the SAR values of the antenna, including the case with the user's hand presence [20–25], are also analyzed.

2. PROPOSED ANTENNA

Figure 1 shows the geometry of the small-size wideband monopole antenna closely coupled with a chip-inductor-loaded shorted strip for the 11-band WWAN/WLAN/WiMAX operation in the slim mobile phone. The antenna with a footprint of $15 \times 20.5 \text{ mm}^2$ ($\sim 308 \text{ mm}^2$) is disposed on the no-ground portion of $15 \times 28 \text{ mm}^2$ of the system circuit board of the mobile phone. Note that owing to the antenna's small size, it is not necessary for the proposed antenna to occupy the entire edge of the system circuit board, which is fabricated using a 0.8-mm thick FR4 substrate of relative permittivity 4.4 and loss tangent 0.024 in this study. In this case, the system ground plane printed on the back side of the circuit board can have an additional protruded ground ($15 \times 22 \text{ mm}^2$) located at the edge of the circuit board. This protruded ground is connected to the main ground ($50 \times 100 \text{ mm}^2$) and can be used to accommodate the associated electronic components in the mobile phone for more efficient board space planning of the system circuit board. This is an advantage over many reported internal WWAN mobile phone antennas that are required to be disposed at the entire edge of the system circuit board [1–5, 26–28]. Also note that to minimize the effect of the protruded ground on the performances of the antenna, a distance of 7.5 mm between the antenna and the protruded ground is required in this study (see Fig. 1).

With a small occupied size, the antenna also shows a simple structure. The antenna is formed by a wideband printed monopole antenna closely coupled with a parasitic chip-inductor-loaded shorted strip. With the printed monopole alone, it can generate a very wide operating band of $>3 \text{ GHz}$ to cover the desired GSM1800/1900/UMTS (1710–2170 MHz), 2.4/4.2/5.8 GHz WLAN bands (2400–5875 MHz), and 2.5/3.5/5.5 GHz WiMAX bands (2500–5850 MHz). Then, by adding the chip-inductor-loaded shorted strip (section BC in the figure) to be closely around the printed monopole such that the shorted strip is closely coupled and capacitively excited by the printed monopole through the coupling gaps indicated in the figure. Although the shorted strip has a length of $\sim 52 \text{ mm}$ only (~ 0.16 wavelength at 900 MHz), a resonant mode with a large operating

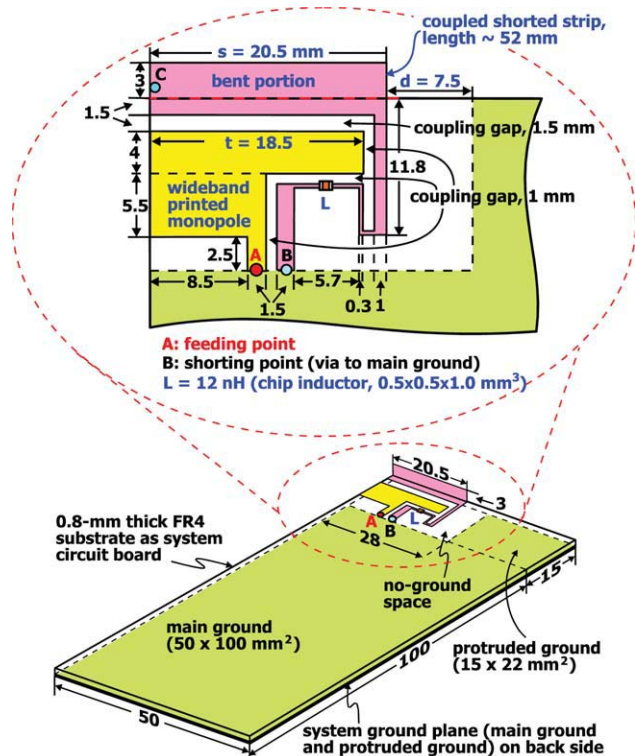
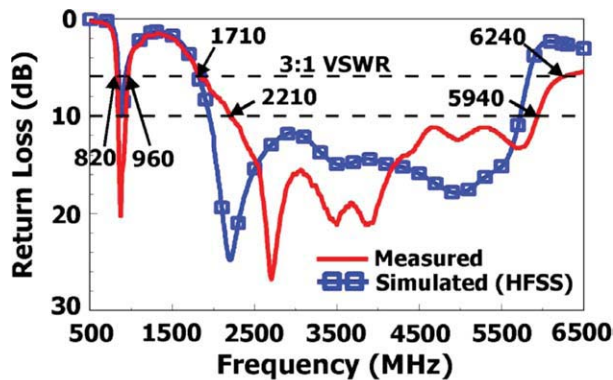


Figure 1 Geometry of the small-size wideband monopole antenna closely coupled with a chip-inductor-loaded shorted strip for WWAN/WLAN/WiMAX operation in the slim mobile phone. [Color figure can be viewed in the online issue, which is available at wileyonlinelibrary.com]

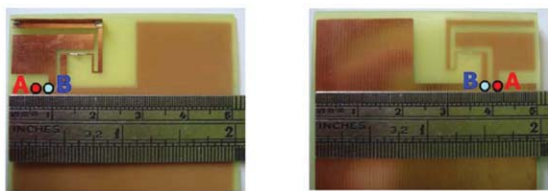
bandwidth to cover the GSM850/900 (824–960 MHz) can be generated. This behavior is attributed to the loaded chip inductor of 12 nH, which effectively compensates for the increased capacitance with the decreasing resonant length of the antenna [29–31]. Also note that the bent portion ($3 \times 20.5 \text{ mm}^2$) increases the width of the open-end section of the shorted strip to be 4.5 mm, which helps enhance the bandwidth of the excited resonant mode. With the bent portion, the antenna shows a thin thickness of 3 mm above the system circuit board. This makes the proposed internal antenna very promising to be applied in the modern slim mobile phones.

3. RESULTS AND DISCUSSION

Based on the design dimensions shown in Figure 1, the proposed antenna was fabricated and tested. The photos of the fabricated antenna are shown in Figure 2(b), and the measured and simulated results are presented in Figure 2(a). The simulated results are obtained using Ansoft HFSS version 12 [32], and good agreement between the measured data and the simulated results is obtained. Two wide operating bands have been obtained for the antenna. The measured bandwidth in the lower band defined by 3:1 VSWR (6-dB return loss) is 140 MHz (820–960 MHz), while the upper bands have a very wide bandwidth of 4530 MHz (1710–6240 MHz). The obtained bandwidth covers the five-band WWAN operation. Further, owing to the large bandwidth and good impedance matching for frequencies over the upper bands, the measured bandwidth defined by 10 dB return loss is 3730 MHz (2210–5940 MHz) and can cover the three-band 2.4/5.2/5.8 GHz WLAN operation and the three-band 2.5/3.5/5.5 GHz WiMAX operation. Hence, the proposed antenna can cover the 11-band WWAN/WLAN/WiMAX operation.



(a)



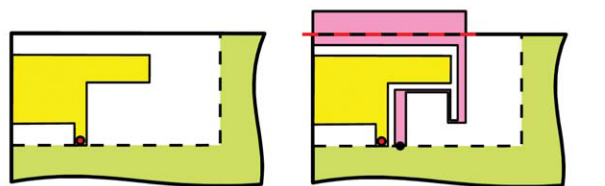
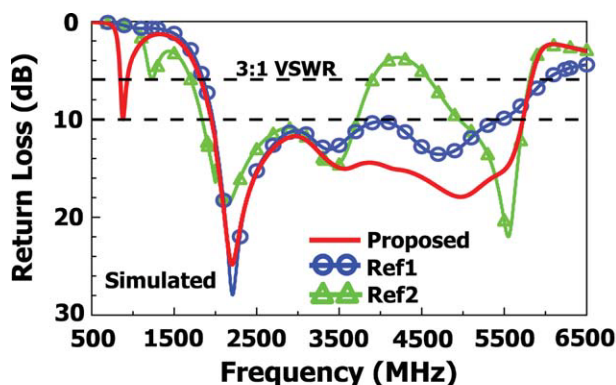
Front view

Back view

(b)

Figure 2 a: Measured and simulated return loss of the proposed antenna. b: Photos of the fabricated antenna. [Color figure can be viewed in the online issue, which is available at wileyonlinelibrary.com]

To analyze the operating principle of the antenna, Figure 3 shows a comparison of the simulated return loss for the proposed antenna, the wideband printed monopole only (Ref1), and the wideband printed monopole closely coupled with a simple shorted strip (Ref2). Note that the corresponding dimensions of



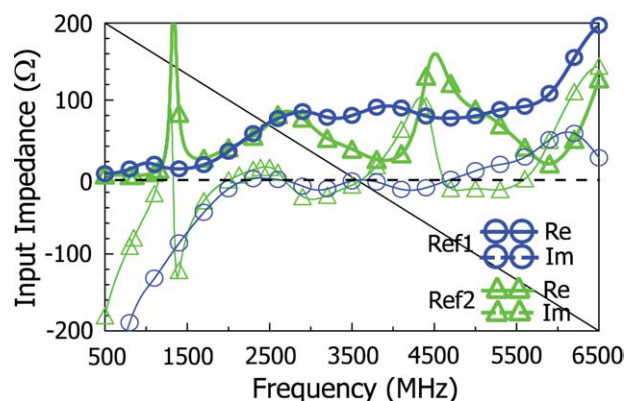
Ref1
(Wideband printed monopole only)

Ref2
(Wideband printed monopole closely coupled with a simple shorted strip)

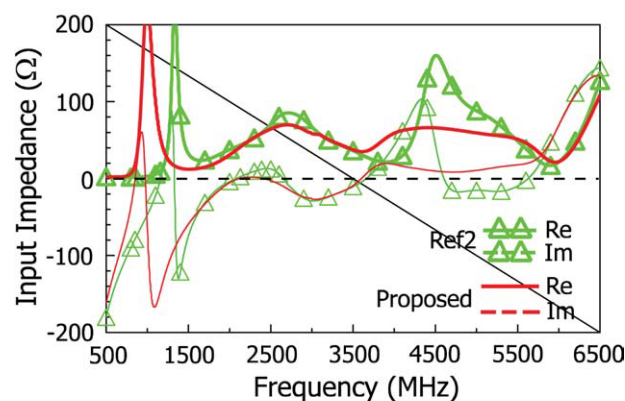
Figure 3 Simulated return loss for the proposed antenna, the wideband printed monopole only (Ref1), and the wideband printed monopole closely coupled with a simple shorted strip (Ref2). [Color figure can be viewed in the online issue, which is available at wileyonlinelibrary.com]

Ref1 and Ref2 are the same as those of the proposed antenna. For Ref1, a wide operating band is generated and generally covers the desired upper band of the proposed antenna. By further adding a simple shorted strip to form Ref2, a new resonant mode at ~ 1200 MHz is generated, with some degraded impedance matching around 4 GHz in the upper band. This new resonant mode can be seen more clearly from the simulated input impedance of Ref2 shown in Figure 4(a). However, the new resonant mode of Ref2 cannot cover the desired GSM850/900 operation. Then, with the presence of the chip inductor of 12 nH in the shorted strip (the proposed antenna), this new resonant mode can be shifted to lower frequencies at ~ 900 MHz and cover the GSM850/900 operation [also see the input impedance of Ref2 and proposed antenna shown in Fig. 4(b)]. This behavior confirms the discussion in Proposed Antenna section for the operating principle of the antenna. In addition, the degraded impedance matching around 4 GHz in the upper band is also greatly improved to achieve a very wide operating band for the antenna's upper band.

Figure 5 shows the simulated surface current distributions for the proposed antenna at 880 and 2200 MHz. At 880 MHz, strong surface current distributions on the coupled shorted strip are seen. This can also confirm that the lower band is mainly contributed by the coupled shorted strip. For the surface current distributions at 2200 MHz, strong surface currents are excited on the printed monopole, which agrees with the observation that the upper band is mainly contributed by the printed monopole as shown in Figures 3 and 4.



(a)



(b)

Figure 4 Simulated input impedance for the three antennas studied in Fig. 3. (a) Ref1 and Ref2. (b) Ref2 and proposed antenna. [Color figure can be viewed in the online issue, which is available at wileyonlinelibrary.com]

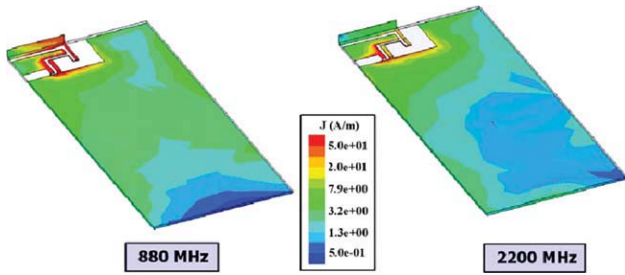
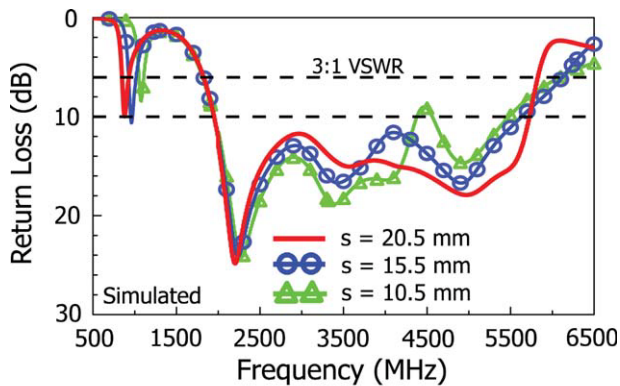


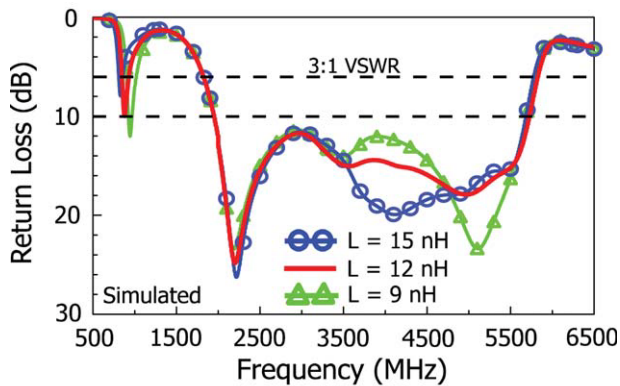
Figure 5 Simulated surface current distributions for the proposed antenna at 880 and 2200 MHz. [Color figure can be viewed in the online issue, which is available at wileyonlinelibrary.com]

Effects of the length s of the widened portion of the coupled shorted strip are studied in Figure 6(a). Simulated results of the return loss for the length s varied from 10.5 to 20.5 mm are presented. Other dimensions are the same as given in Figure 1. When the length s is increased, the resonant mode for the antenna's lower band is shifted to lower frequencies. Figure 6(b) shows the effects of the loaded chip inductor. Simulated results of the return loss for the inductance L varied from 9 to 15 nH are presented. Again, the resonant mode for the antenna's lower band is shifted to lower frequencies for increasing inductance. The results indicate that by adjusting the length s and the inductance L , the antenna's lower band can be easily controlled.

Figure 7 shows the effects of the width t of the wideband printed monopole. Simulated results of the return loss for the



(a)



(b)

Figure 6 Simulated return loss as a function of (a) the length s of the widened portion of the coupled shorted strip and (b) the values of the chip inductor L . Other dimensions are the same as given in Fig. 1. [Color figure can be viewed in the online issue, which is available at wileyonlinelibrary.com]

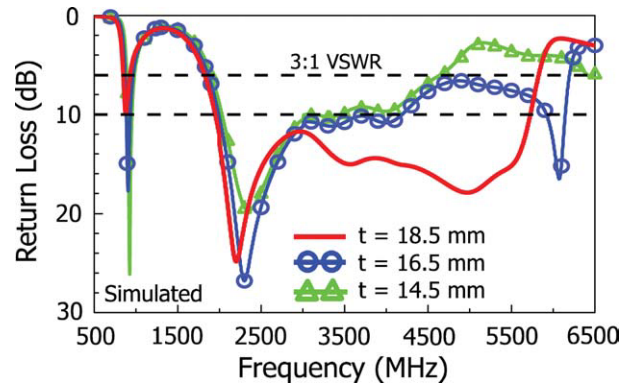


Figure 7 Simulated return loss as a function of the width t of the wideband printed monopole. Other dimensions are the same as given in Fig. 1. [Color figure can be viewed in the online issue, which is available at wileyonlinelibrary.com]

width t varied from 14.5 to 18.5 mm are presented. Large effects on the antenna's upper band are seen, especially at higher frequencies of the upper band. The obtained bandwidth of the upper band is decreased with a decrease in the width t . This is mainly because the achievable operating bandwidth of the printed or planar monopole is greatly dependent on the width of the monopole, which is similar to the observations for the ultra-wideband planar monopole antennas [33, 34]. To achieve a very wide operating band for the antenna's upper band, a large width t of 18.5 mm is selected in this study.

Effects of the distance d between the antenna and the protruded ground are analyzed in Figure 8. Results of the simulated return loss for the distance d varied from 1.5 to 7.5 mm are presented. When the distance d is decreased, the impedance matching for frequencies over the antenna's lower and upper bands is degraded. Hence, an isolation distance of 7.5 mm is required in this study to minimize the effects of the protruded ground on the performances of the proposed antenna.

Figure 9 shows the measured three-dimensional total-power radiation patterns for the fabricated antenna. At each frequency, three radiation patterns seen in different directions are shown. For the lower frequency at 859 MHz, the radiation patterns are similar to those of a conventional half-wavelength dipole antenna. For higher frequencies, the radiation patterns become more directive. In addition, as the antenna is disposed at one corner of the system circuit board and is asymmetric with

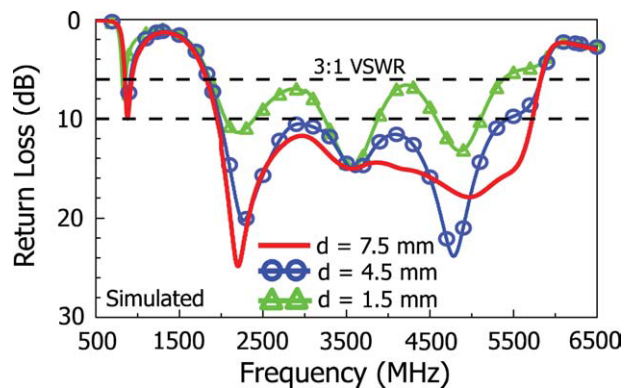


Figure 8 Simulated return loss as a function of the distance d between the proposed antenna and the protruded ground. Other dimensions are the same as given in Fig. 1. [Color figure can be viewed in the online issue, which is available at wileyonlinelibrary.com]

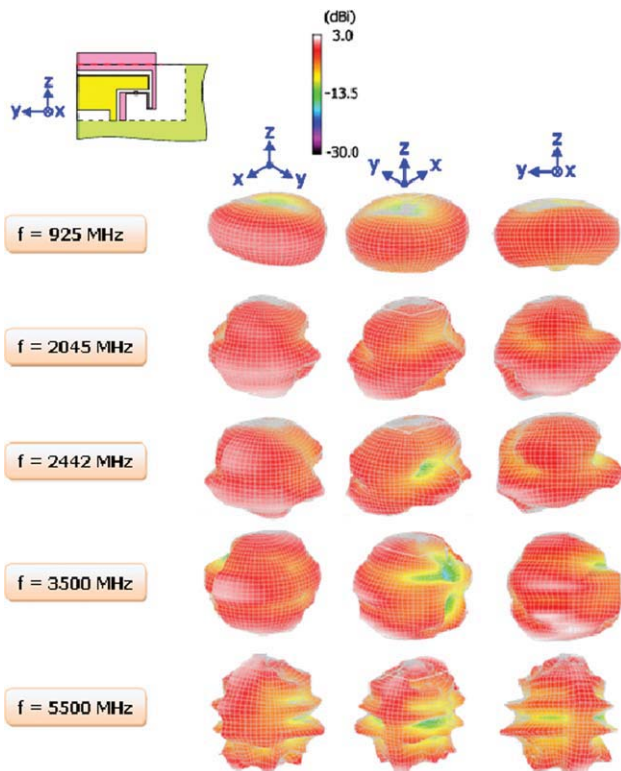


Figure 9 Measured three-dimensional total-power radiation patterns for the fabricated antenna. [Color figure can be viewed in the online issue, which is available at wileyonlinelibrary.com]

respect to the centerline of the system ground plane, the radiation patterns also show some asymmetries with respect to the z axis. The measured radiation efficiency and antenna gain are shown in Figure 10. The measured radiation efficiency over the lower and upper bands is, respectively, about 52–72% and 58–80%. The measured gain is about -0.6 to 0.8 dBi and 1.2 – 5.0 dBi over the lower and upper bands, respectively. Good radiation characteristics are generally obtained for the proposed antenna.

The SAR results of the proposed antenna for the five-band WWAN operation are studied using the SAR simulation models provided by SEMCAD X version 14.2 [35]. Figure 11 shows the SAR simulation model and the simulated SAR values. Both the hand and head phantoms are considered, and the delivered power for the lower band (859 and 925 MHz) and upper band (1795, 1920, and 2045 MHz) is 24 and 21 dBm, respectively. As it is well known that this kind of wideband internal antenna without a ground plane on back is suitable to be positioned at the bottom of the mobile phone to achieve decreased SAR values [7, 20, 27, 29], the proposed antenna in the SAR testing is also positioned at the bottom of the mobile phone. The distance between the system ground plane and the palm center of the hand phantom is 35 mm. From the results, the obtained 1 g SAR values for the head only are 0.49–1.41 W/kg for the five WWAN operating bands and are lower than the limit of 1.6 W/kg required for practical mobile phone applications [11]. When the hand is present, small variations in the SAR values are seen for the lower band. However, for the upper band, there are strong effects on the SAR values. Notice that for the upper band, the SAR values with the head and hand presence are three times higher than those with the head only. This behavior needs to be considered when the user's hand is to be included in the

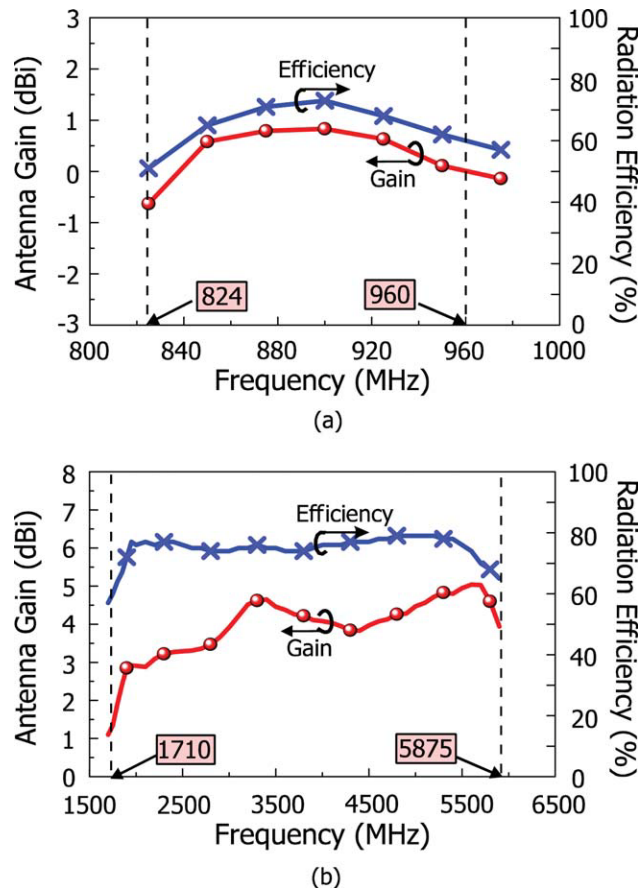
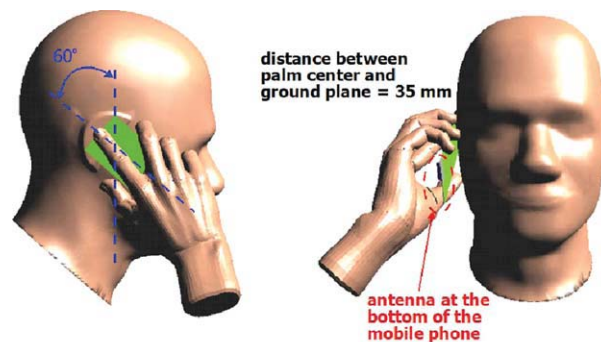


Figure 10 Measured radiation efficiency and antenna gain for the fabricated antenna. (a) The lower band (824–960 MHz). (b) The upper band (1710–5875 MHz). [Color figure can be viewed in the online issue, which is available at wileyonlinelibrary.com]



Frequency (MHz)		859	925	1795	1920	2045
Delivered power (Watt)		24 dBm		21 dBm		
1-g SAR (Watt/kg)	head only	1.09	1.41	0.49	0.59	0.63
	head and hand	1.41	1.49	1.81	2.02	2.06
Return loss (dB)	head only	7.2	8.3	6.5	10.9	16.7
	head and hand	10.0	10.4	8.6	13.0	18.4

Figure 11 SAR simulation model provided by SEMCAD X and the simulated SAR values. The return loss shown in the table is the impedance matching level at the testing frequency. [Color figure can be viewed in the online issue, which is available at wileyonlinelibrary.com]

SAR specifications for the internal mobile phone antennas in the future [20].

4. CONCLUSION

A promising small-size internal mobile phone antenna suitable for the 11-band WWAN/WLAN/WiMAX operation has been proposed. The antenna has a simple structure and is formed by a wideband printed monopole antenna closely coupled with a chip-inductor-loaded shorted strip. The antenna provides two wide operating bands for the desired 11-band operation, with the lower and upper bands easily controlled by the printed monopole and the shorted strip, respectively. In addition to the small size occupied on the system circuit board, the antenna also shows a small thickness of 3 mm only, which makes it very promising for modern slim mobile phone applications. Good radiation characteristics over the operating bands have also been obtained. The simulated 1 g SAR results for the proposed antenna positioned at the bottom of the mobile phone with the head only are well below the 1.6 W/kg limit, making the proposed antenna very promising for practical mobile phone applications. However, when both the head and hand are included in the SAR testing, the obtained SAR values are three times higher than those with the head only for operating in the GSM1800/1900/UMTS bands. When both the head and hand are required for the SAR testing in the near future [20], this behavior needs to be considered for the practical applications of the proposed antenna.

REFERENCES

1. W.Y. Chen and K.L. Wong, Small-size coupled-fed shorted T-monopole for internal WWAN antenna in the slim mobile phone, *Microwave Opt Technol Lett* 52 (2010), 257–262.
2. K.L. Wong and W.Y. Chen, Small-size printed loop antenna for penta-band thin-profile mobile phone application, *Microwave Opt Technol Lett* 51 (2009), 1512–1517.
3. R.A. Bhatti, Y.T. Im, J.H. Choi, T.D. Manh, and S.O. Park, Ultrathin planar inverted-F antenna for multistandard handsets, *Microwave Opt Technol Lett* 50 (2008), 2894–2897.
4. H. Rhyu, J. Byun, F.J. Harakiewicz, M.J. Park, K. Jung, D. Kim, N. Kim, T. Kim, and B. Lee, Multi-band hybrid antenna for ultrathin mobile phone applications, *Electron Lett* 45 (2009), 773–334.
5. R.A. Bhatti and S.O. Park, Octa-band internal monopole antenna for mobile phone applications, *Electron Lett* 44 (2008), 1447–1448.
6. C.T. Lee and K.L. Wong, Uniplanar coupled-fed printed PIFA for WWAN/WLAN operation in the mobile phone, *Microwave Opt Technol Lett* 51 (2009), 1250–1257.
7. C.H. Chang and K.L. Wong, Printed $\lambda/8$ -PIFA for penta-band WWAN operation in the mobile phone, *IEEE Trans Antennas Propagat* 57 (2009), 1373–1381.
8. C.T. Lee and K.L. Wong, Internal WWAN clamshell mobile phone antenna using a current trap for reduced groundplane effects, *IEEE Trans Antennas Propagat* 57 (2009), 3303–3308.
9. T.W. Kang and K.L. Wong, Simple small-size coupled-fed uniplanar PIFA for multiband clamshell mobile phone application, *Microwave Opt Technol Lett* 51 (2009), 2805–2810.
10. K.L. Wong and W.Y. Chen, Small-size printed loop-type antenna integrated with two stacked coupled-fed shorted strip monopoles for eight-band LTE/GSM/UMTS operation in the mobile phone, *Microwave Opt Technol Lett* 52 (2010), 1471–1476.
11. American National Standards Institute (ANSI), Safety levels with respect to human exposure to radio-frequency electromagnetic field, 3 kHz to 300 GHz, ANSI/IEEE standard C95.1 (1999).
12. T. Yang, W. A. Davis, W. L. Stutzman, and M. C. Huynh, Cellular-phone and hearing-aid interaction: an antenna solution, *IEEE Antennas Propagat Mag* 50 (2008), 51–65.
13. C.T. Lee and K.L. Wong, Uniplanar printed coupled-fed PIFA with a band-notching slit for WLAN/WiMAX operation in the lap-

- top computer, *IEEE Trans Antennas Propagat* 57 (2009), 1252–1258.
14. L.C. Chou and K.L. Wong, Uni-planar dual-band monopole antenna for 2.4/5 GHz WLAN operation in the laptop computer, *IEEE Trans Antennas Propagat* 55 (2007), 3739–3741.
15. C.M. Su, W.S. Chen, Y.T. Cheng, and K.L. Wong, Shorted T-shaped monopole antenna for 2.4/5 GHz WLAN operation, *Microwave Opt Technol Lett* 41 (2004), 202–203.
16. Worldwide interoperability for microwave access forum or WiMAX forum, available at: <http://www.wimaxforum.org>.
17. K.L. Wong and P.Y. Lai, Wideband integrated monopole slot antenna for WLAN/WiMAX operation in the mobile phone, *Microwave Opt Technol Lett* 50 (2008), 2000–2005.
18. P.Y. Lai and K.L. Wong, Capacitively-fed hybrid monopole/slot antenna for 2.5/3.5/5.5 GHz WiMAX operation in the mobile phone, *Microwave Opt Technol Lett* 50 (2008), 2689–2694.
19. M.R. Hsu and K.L. Wong, Seven-band folded-loop chip antenna for WWAN/WLAN/WiMAX operation in the mobile phone, *Microwave Opt Technol Lett* 51 (2009), 543–549.
20. C.H. Li, E. Offi, N. Chavannes, and N. Kuster, Effects of hand phantom on mobile phone antenna performance, *IEEE Trans Antennas Propagat* 57 (2009), 2763–2770.
21. C.M. Su, C.H. Wu, K.L. Wong, S.H. Yeh, and C.L. Tang, User's hand effects on EMC internal GSM/DCS dual-band mobile phone antenna, *Microwave Opt Technol Lett* 48 (2006), 1563–1569.
22. C.I. Lin, K.L. Wong, S.H. Yeh, and C.L. Tang, Study of an L-shaped EMC chip antenna for UMTS operation in a PDA phone with the user's hand, *Microwave Opt Technol Lett* 48 (2006), 1746–1749.
23. C.I. Lin and K.L. Wong, Printed monopole slot antenna for internal multiband mobile phone antenna, *IEEE Trans Antennas Propagat* 55 (2007), 3690–3697.
24. C.I. Lin and K.L. Wong, Internal meandered loop antenna for GSM/DCS/PCS multiband operation in a mobile phone with the user's hand, *Microwave Opt Technol Lett* 49 (2007), 759–765.
25. C.T. Lee and K.L. Wong, Study of a uniplanar printed internal WWAN laptop computer antenna including user's hand effects, *Microwave Opt Technol Lett* 51 (2009), 2341–2346.
26. K.L. Wong and S.C. Chen, Printed single-strip monopole using a chip inductor for penta-band WWAN operation in the mobile phone, *IEEE Trans Antennas Propagat* 58 (2010), 1011–1014.
27. Y.W. Chi and K.L. Wong, Quarter-wavelength printed loop antenna with an internal printed matching circuit for GSM/DCS/PCS/UMTS operation in the mobile phone, *IEEE Trans Antennas Propagat* 57 (2009), 2541–2547.
28. Y.W. Chi and K.L. Wong, Compact multiband folded loop chip antenna for small-size mobile phone, *IEEE Trans Antennas Propagat* 56 (2008), 3797–3803.
29. T.W. Kang and K.L. Wong, Chip-inductor-embedded small-size printed strip monopole for WWAN operation in the mobile phone, *Microwave Opt Technol Lett* 51 (2009), 966–971.
30. J. Carr, *Antenna toolkit*, 2nd ed., Newnes, Oxford, UK, 2001, pp. 111–112.
31. J. Thaysen and K. B. Jakobsen, A size reduction technique for mobile phone PIFA antennas using lumped inductors, *Microwave J* 48 (2005), 114–126.
32. Ansoft Corporation HFSS, available at: <http://www.ansoft.com/products/hf/hfss/>.
33. K.L. Wong, C.H. Wu, and S.W. Su, Ultra-wideband square planar metal-plate monopole antenna with a trident-shaped feeding strip, *IEEE Trans Antennas Propagat* 53 (2005), 1262–1269.
34. K.L. Wong, S.W. Su, and C.L. Tang, Broadband omnidirectional metal-plate monopole antenna, *IEEE Trans Antennas Propagat* 53 (2005), 581–583.
35. SEMCAD, Schmid and Partner Engineering AG (SPEAG), available at: <http://www.semcad.com>.